09

Photodissociation iodine laser with a variable directional pattern and output energy of 10 J

© G.N. Kachalin, 1,2 A.D. Malakhov, 1,2 E.A. Salatov, 1,2 O.L. Techko 1,2

¹Russian Federal Nuclear Center All-Russian Research Institute of Experimental Physics,

607188 Sarov, Nizhny Novgorod Oblast, Russia

²Sarov Branch of Lomonosov Moscow State University,

607328 Sarov, Nizhny Novgorod Oblast, Russia

e-mail: info@sarov.msu.ru

Received August 6, 2024 Revised May 12, 2025 Accepted May 12, 2025

We have created a powerful photodissociation iodine laser with a variable directional pattern, which is designed to operate in a free generation mode. Its design includes a conjugate resonator and a light spatiotemporal modulation device based on the electrooptical ceramics of the lanthanum-doped plumbum zirconate-titanate composition. The laser generation energy was (9.1 ± 0.7) J at the pulse duration of $175\,\mu s$ and radiation divergence of $5 \cdot 10^{-4}$ rad. It is demonstrated that the inter-resonator spatiotemporal light modulator withstands beam loads of $6.8 \cdot 10^6$ W/cm².

Keywords: iodine laser, photodissociation, free generation mode, conjugate resonator, spatiotemporal modulator.

DOI: 10.61011/TP.2025.08.61740.250-24

Introduction

In various applications of the lasers, a relevant task is to control the directional pattern of output radiation. This task is solved by applying inter-resonator spatiotemporal light modulation (STLM) [1–4]. The paper [5] was the first to propose and implement application of STLM based on the electrooptical ceramics of the lanthanum-doped plumbum zirconate-titanate (LPZT). The STLM diagram based on two orthogonal half-wave shutters makes it possible to effectively control the directional pattern within the whole field of view of the laser [6], while ensuring a required spatial contrast of radiation [6]. The present study has created the photodissociation iodine laser with the inter-resonator high-contrast STLM diagram, which has radiation output energy $(9.1\pm0.7)\,\rm J.$

1. Optical laser layout

Fig. 1 shows the optical layout of the laser resonator and its photo of a quartz cuvette in a cylindrical lighter with pumping lamps. Technical characteristics of the iodine laser are shown in the table. The conjugate resonator with a kink of the optical axis. It consisted of two flat mirrors R_b and R_f that are arranged in focal planes of confocal lenses F_1 and F_2 . Radiation was output from the resonator by a semitransparent flat mirror.

The laser quartz cuvette was placed in the cylindrical lighter. Cuvette windows were made of the K8 glass at the Brewster angle. An active medium was pumped by 20 pump-out lamps that are filled with xenon at the pressure of 330 Torr and placed inside the lighter. The entire structure was fixed on two supports of the height of 950 mm.

For dielectric insulation the support parts were made of caprolon. Xenon was supplied into the lamps through a splitter connected to each lamps with its own pipeline. The cuvette was connected to the pump-out system by means of pipelines, stoppers and valves. The working mixture was a mixture $n\text{-}C_3F_7I + \text{argon 1:10}$ at the total pressure of 24 Torr. This mixture is optimal in terms of output energy and homogeneity of the near zone of a master oscillator [7].

The experiments were carried out in the following sequence: obtaining free generation in the resonator with the angular selector as a rigid diaphragm, obtaining free generation in the STLM resonator.

Study of radiation characteristics of the laser with the inter-resonator model diaphragm of the angular selector

With placing the lens of the angular selector of the model diaphragm with the diameter $d=4\,\mathrm{mm}$ into the focal plane, the generation energy $E_{gen}=(11.0\pm0.3)\,\mathrm{J}$ was obtained. The generation oscillogram is shown in Fig. 2, a. The measured generation energy was taken to determine the energy stored in the active medium and its density in accordance with the relationships

$$E_{stor} = \frac{h\nu}{\sigma} S \ln\left(\frac{1}{\sqrt{R_1 R_2}}\right) + \frac{E_{gen}}{R_{outp}} \left(1 - R_2\right) + \left(1 - R_1\right) \sqrt{\frac{R_1}{R_2}} = 41 J,$$
(1)

$$\varepsilon_{stor} = E_{stor} \cdot \frac{4}{\pi D_a^2 L_a} = 10.4 \,\mathrm{mJ/cm}^3,$$
 (2)

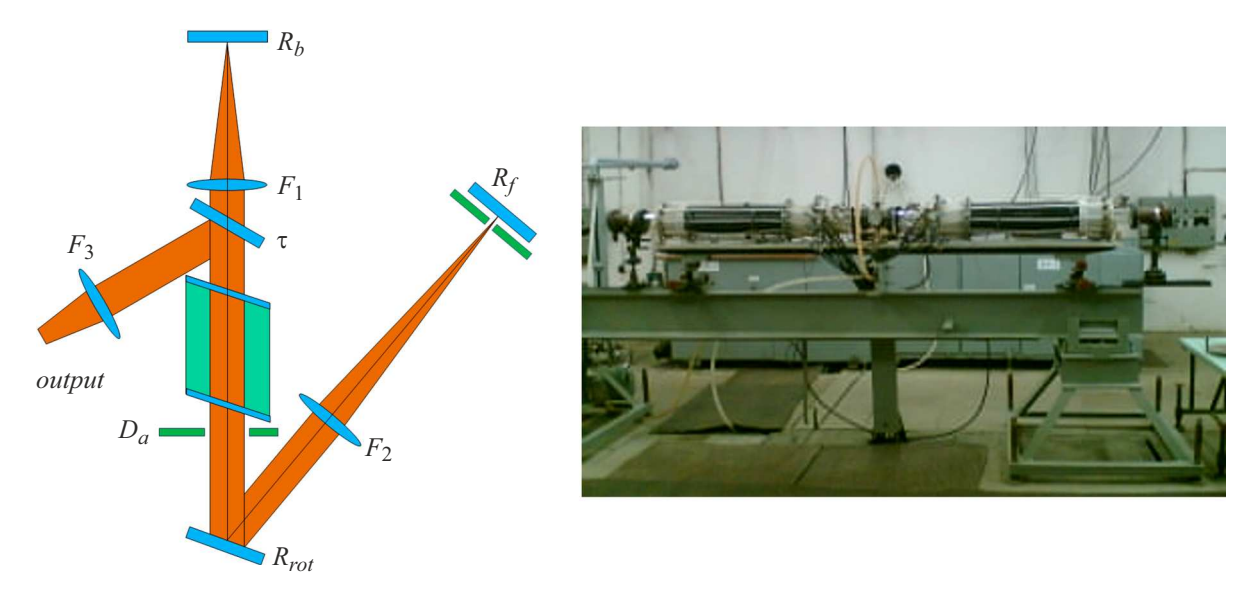


Figure 1. Photodissociation iodine laser.

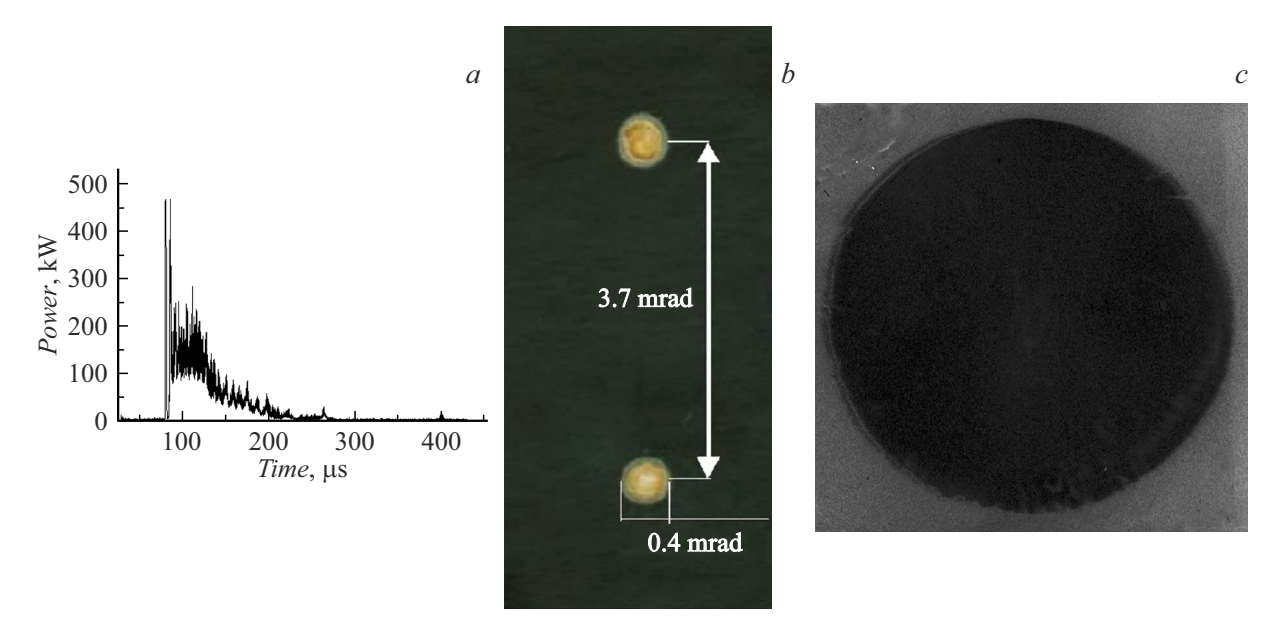


Figure 2. Generation oscillogram (a), the far-zone radiation pattern from two successive pulses when moving a diaphragm within a focal plane of the angular selector lens (b) and the near-zone radiation pattern (c).

where $R_1=0.069$, $R_2=0.568$ — the effective reflectances of the rear and the front mirrors of the resonator, $h\nu=1.51\cdot 10^{-19}\,\mathrm{J}$ — the energy of the laser quantum, $R_{outp}=0.6$ — the effective reflectance of the output mirror, $E_{thresh}=\frac{h\nu}{\sigma}\,S\ln\left(\frac{1}{\sqrt{R_1R_2}}\right)$ — the threshold energy of generation development [8], $S=\frac{\pi D_a^2}{4}$ — the active medium's section area, D_a — the aperture diaphragm diameter, L_a — the cuvette's active length, $\sigma=4.69\cdot 10^{-18}\,\mathrm{cm}^2$ — the section of amplification of the laser medium.

The patterns of radiation in the far- and the nearzones were recorded by using an additional extraresonator lens with the focal distance $F_3 = 5.12 \,\mathrm{m}$ (Fig. 1) and a calibrated set of light filters. The far-zone radiation imprints when moving the angular selector diaphragm into extreme positions that are spaced by $\Delta L = 37 \,\mathrm{mm}$ and limited by a size of an STLM working field $D_{STLM} = 40 \,\mathrm{mm}$ were recorded as burns on the photopaper (Fig. 2, b). The near-zone radiation pattern was recorded on the IR photofilm (Fig. 2, c).

Fig. 3 shows the dependence of the rated energy of a diaphragm shift from the resonator axis.

It is clear from Fig. 3 that at an edge of the working field limited by the STLM size the energy generation drop is below 11%.

Intra-resonator scanning of the laser radiation direction was carried out by moving the square diaphragm 5×5 mm within the focal plane of the angular selector lens with $F_2 = 10.02$ m without readjusting the resonator. The farzone radiation patterns are shown in Fig. 4.

Based on the results of the performed experiments, it can be concluded that all the optical elements included in the resonator withstand the beam loads at the generation energy of $\sim 10\,\mathrm{J}$ when scanning across the whole field of view of the laser [6]. The generation energy is insignificantly reduced when operating at the edges of the STLM working field, which is related to vignetting effects. The diagram for measuring angular radiation energy distribution is shown in Fig. 5.

According to a series of the pulses, the calorimeters 5 and 6 were calibrated to each other. Then, the diaphragms of a various diameter were placed in front of the calorimeter 5

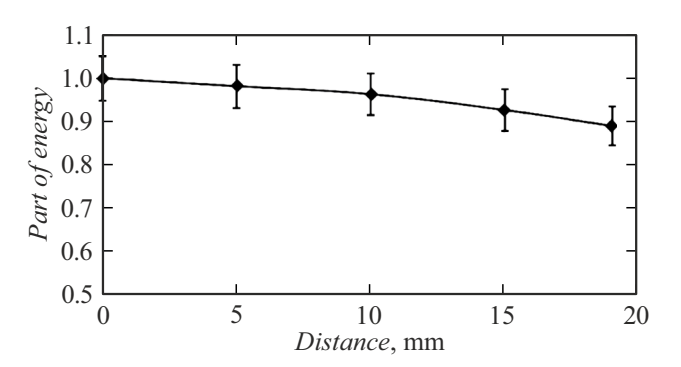


Figure 3. Dependence of the rated energy on the position of the selecting diaphragm in relation to the resonator axis.

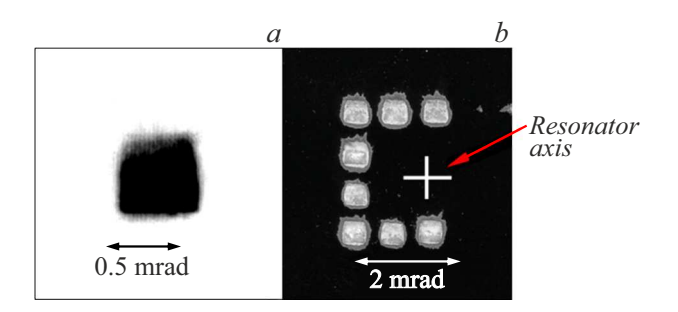


Figure 4. Far-zone radiation patterns: a — the single pulse, b — the eight successive pulses without readjusting the resonator.

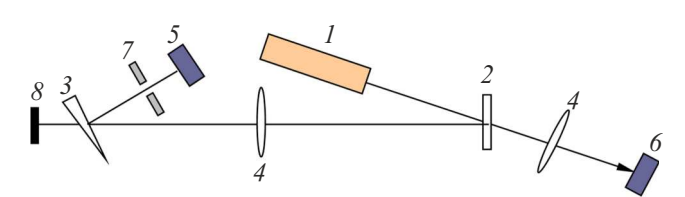


Figure 5. Optical layout for measuring angular energy distribution: I — the iodine laser, 2 — the beam splitter mirror, 3 – the wedge, 4 — the reconfiguring lenses, 5 — the calorimeter, 6 — the reference calorimeter, 7 — the square diaphragm $(2.5 \times 2.5 \text{ mm}, 7.5 \times 7.5 \text{ mm})$, 8 — the far-zone recording.

in the focal plane of the lens 4 and a part of energy entering a certain angle was determined by means of measurements and recalculation. The angular distribution of energy of generation of the laser with the conjugate resonator the rigid diaphragm 5×5 mm in the focal plane of the angular selector lens is shown in Fig. 6.

Based on the results of measurements, the angle limited by the angular selector size includes $(83\pm2)\,\%$ of the energy.

Study of radiation characteristics of the iodine laser with the inter-resonator STLM

Operation of the iodine laser was experimentally studied as per the diagram of Fig. 7. The laser resonator included a high-contrast STLM circuit with double rotation of the

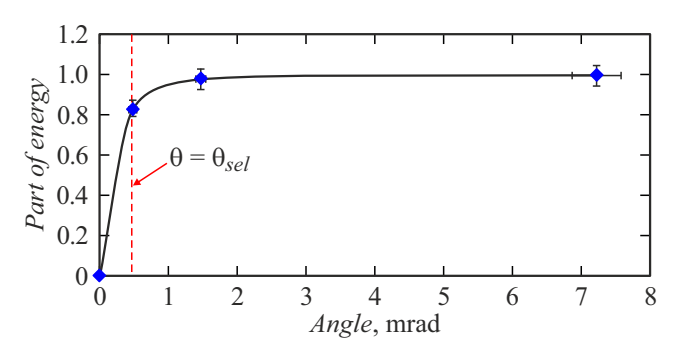


Figure 6. Angular distribution of energy of generation of the laser with the rigid diaphragm 5×5 mm of the angular selector.

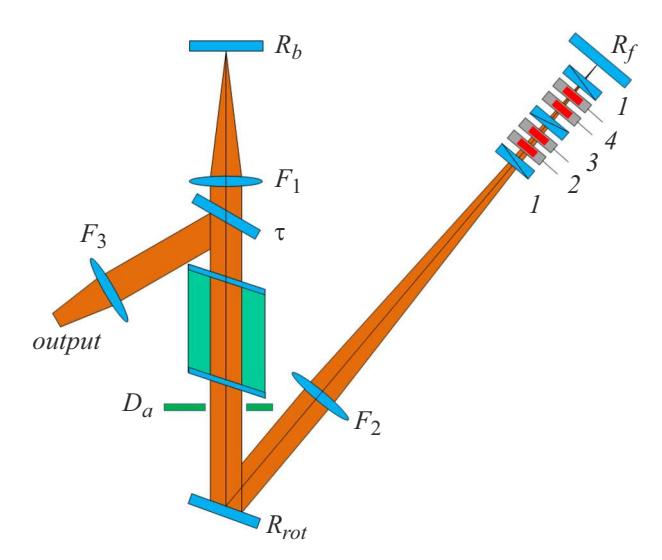


Figure 7. Layout of the iodine lase with the inter-resonator STLM: I — the polarizers with transmittance azimuth of $+45^{\circ}$, 2 — the paired plates made of the electrooptical ceramics along the coordinate x (the quarter-wave voltage in each), 3 — the polarizer with the transmittance azimuth of -45° , 4 — the paired plates made of the electrooptical ceramics along the coordinate y (the quarter-wave voltage in each).

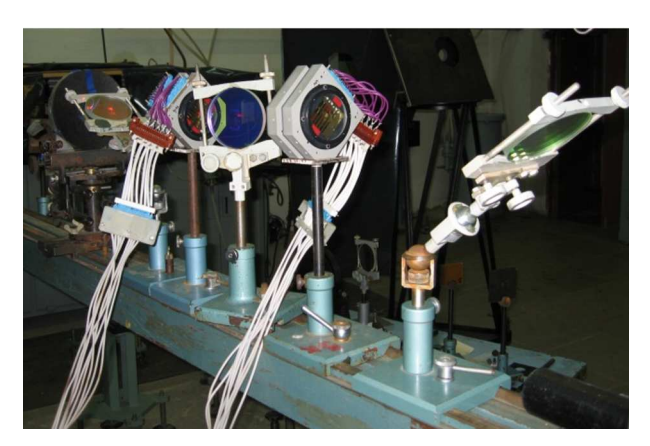


Figure 8. Photo of the STLM with double rotation of the polarization plane by 90° .

polarization plane by 90° , which consisted of the two orthogonal half-wave shutters [6]. The STLM was controlled by an electronic key unit that was connected by hardware to a computer. The photo of the inter-resonator STLM is shown in Fig. 8.

The expected generation energy is evaluated as

$$E_{gen} = \frac{R_{out} \left(E_{stor} - \frac{hv}{\sigma} S \ln \left(\frac{1}{R_1 R_2} \right) \right)}{1 - R_2 + (1 - R_1) \sqrt{\frac{R_1}{R_2}}} = 10.7 \,\text{J}, \quad (3)$$

where $E_{stor} = 41 \, \mathrm{J}$ — the stored energy (see the formula (1)), R_{out} — the reflectance of the output mirror, $S = \frac{\pi D_a^2}{4}$ — the section area of the active medium with the diameter D_a , $\sigma = 4.69 \cdot 10^{-18} \, \mathrm{cm}^2$ — the section of amplification of the laser medium, R_1 , R_2 — the effective reflectances of the front and the rear mirror of the resonator, which are determined by the relationships

$$R_1 = \tau_0^2 R_{rot}^2 \tau_1^2 \tau_{O1}^2 R_f = 0.144, \tag{4}$$

$$R_2 = \tau_0^2 \tau_{out}^2 \tau_1^2 R_b = 0.0689, \tag{5}$$

$$R_{outp} = \tau_0 R_{out} = 0.599,$$
 (6)

where R_b , R_f — the reflectances of the rear and the front mirrors of the resonator (see the table), $\tau_{O1} = 0.503$ — the transmittance of the STLM cell, $\tau_0 = 0.921$ — the transmittance of the cuvette window, $\tau_l = 0.909$ — the transmittance of the lens, $R_{rot} = 0.96$ — the reflectance of the rotatable mirror, $R_{out} = 0.65$, $\tau_{out} = 0.32$ — the reflectance and the transmittance coefficient of the output mirror.

There were about 350 experiments with opening various cells within the whole STLM working field. The average generation energy was $E_{gen}=(9.1\pm0.7)\,\mathrm{J}$, which is close to the calculated value.

The part of energy, which belongs to various recording angles, was measured. The optical layout of arrangement of the calorimeters is similar to that shown in Fig. 5. The angular distribution of the energy of radiation of the laser with the conjugate resonator that contains the STLM with double rotation of the polarization plane by 90° is shown in Fig. 9.

Based on the results of measurements, the angle limited by the angular selector size includes $(81\pm3)\%$ of the energy.

The generation oscillogram is shown in Fig. 10. Fig. 11 shows the radiation patterns with serial switching-on of the STLM cells in several tests.

Photometering of the images d and e (Fig. 11) resulted in obtaining the value of spatial contrast, $\gamma \approx 625$, of the switched-on STLM cell in relation to the remaining working field. In an approximation of counter wave balance in the resonator, the average intensity of laser radiation at the STLM was

$$I = \frac{E_{gen}}{t} \sqrt{\frac{R_1}{R_2}} \frac{\tau_0 \tau_1 R_{rot}}{R_{out} S_c} = 4.3 \cdot 10^5 \text{ W/cm}^2, \tag{7}$$

where $R_1 = 0.144$, $R_2 = 0.0689$ — the effective reflectances of the rear and the front mirrors of the resonator, $\tau_0 = 0.921$ — the transmittance of the cuvette window, $\tau_l = 0.909$ — the transmittance of the lens, $R_{rot} = 0.96$ — the reflectance of the rotatable mirror, $R_{out} = 0.65$ — the reflectance of the output mirror, t — the duration of

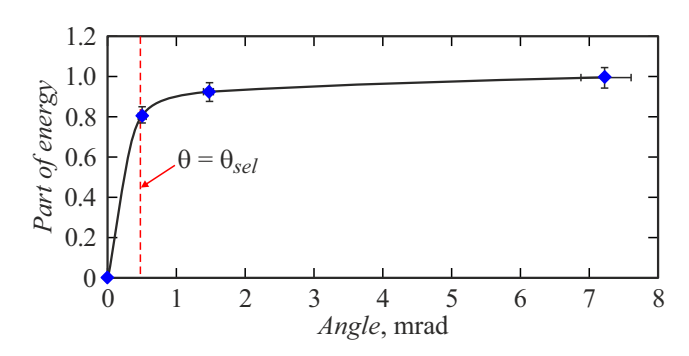


Figure 9. Angular distribution of the energy of radiation of the laser with the conjugate resonator that contains the STLM with double rotation of the polarization plane by 90° .

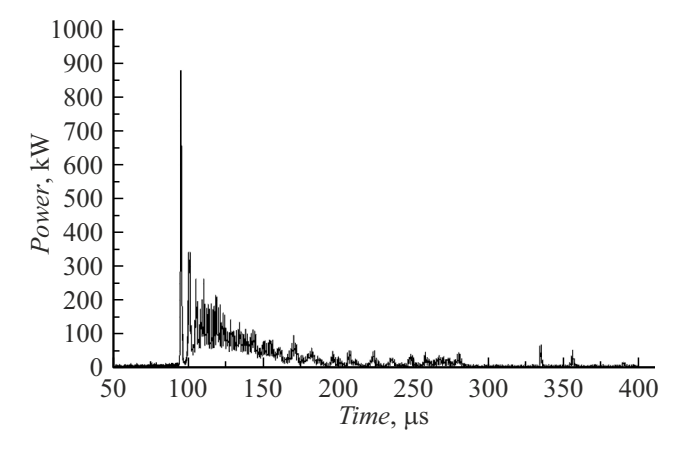


Figure 10. Oscillogram of laser generation.

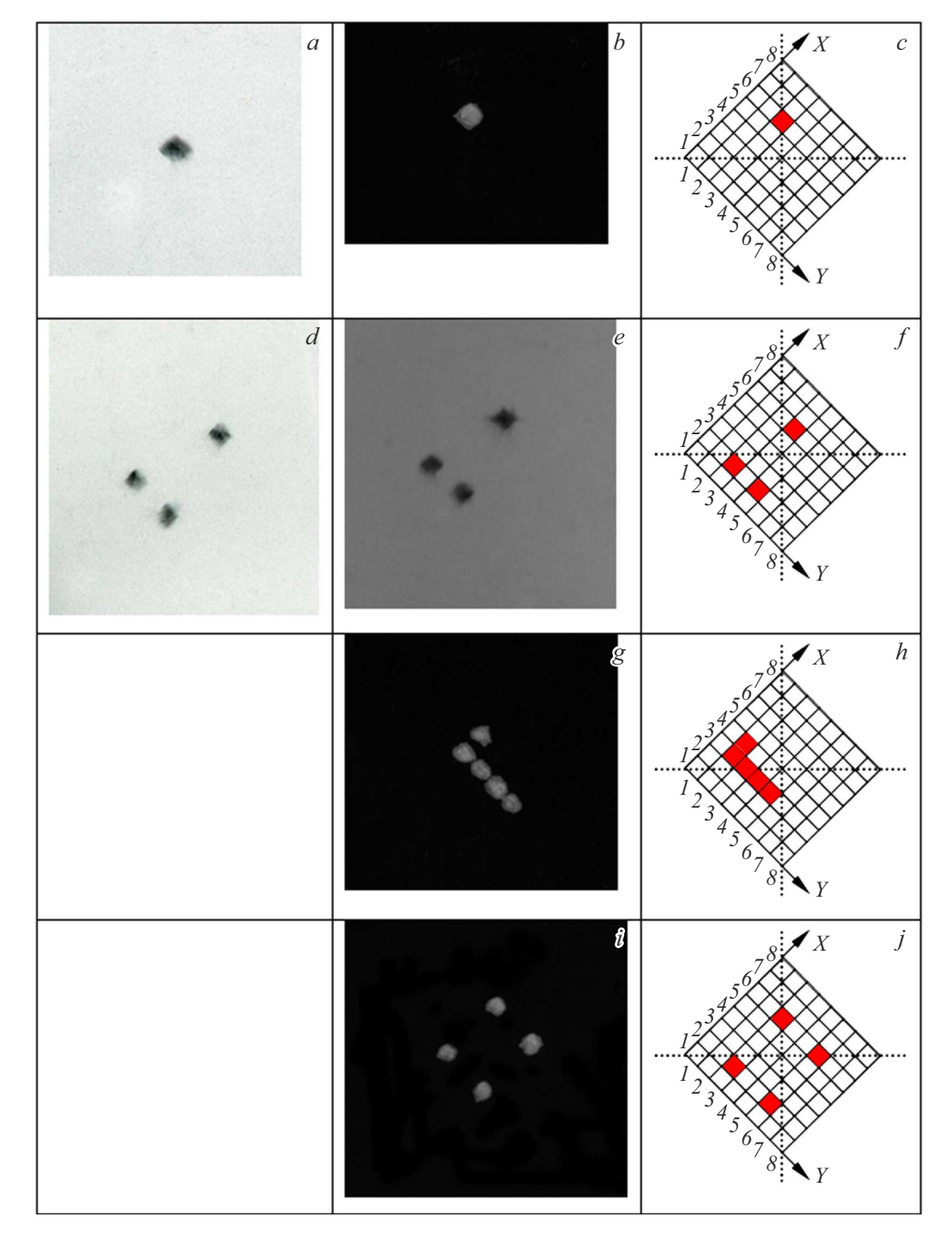


Figure 11. Distribution of a density of blackening or burns in the far zone when switching on the various STLM cells.

generation, $S_c = 0.25 \, \text{cm}^2$ — the area of the elementary STLM cell.

The highest peak value of power of generation of the laser with the STLM-variable directional pattern was $P_{\rm max}=878\,{\rm kW}$ (Fig. 10) and the maximum intensity of radiation incident to the STLM was

$$I_{\text{max}} = P_{\text{max}} \sqrt{\frac{R_1}{R_2}} \frac{\tau_0 \tau_1 R_{rot}}{R_{out} S_c} = 6.8 \cdot 10^6 \,\text{W/cm}^2.$$
 (8)

The obtained value of the maximum intensity of radiation on the STLM elements does not exceed a fracture threshold of an antireflection dielectric coating on the electrooptical ceramics, which is $I_{mod}^{bloom} \approx 10^7 \, \text{W/cm}^2$.

Conclusions

Thus, the studies have resulted in creating a powerful photodissociation iodine laser with the variable directional pattern and it was experimentally demonstrated that inclusion of the STLM in the resonator allowed obtaining output radiation with spatial contrast $\gamma \approx 625$. The output laser energy was $(9.1 \pm 0.7)\,\mathrm{J}$ at radiation divergence of $5\cdot 10^{-4}\,\mathrm{rad}$ and the generation pulse duration of $175\,\mu\mathrm{s}$. We note that these results are obtained in conditions of the beam loads that are close to those which are implemented the master oscillator based on a quartz HPDL option [9,10].

Due to simpleness of interfacing with a computer or a dedicated microprocessor, the photodissociation iodine laser with the electrically-controlled STLM can be widely applied in tasks of object location and in various technological installations [3,11]. The described laser with inter-resonator control of the directional pattern can be used as a master oscillator of the laser systems, including with wavefront conjugation devices [2,12].

Conflict of interest

The authors declare that they have no conflict of interest.

References

- A.A. Vasil'ev, D. Kasasent, I.N. Kompanets, A.V. Parfenov. Prostranstvennye modulyatory sveta (Radio i svyaz', M., 1987) (in Russian).
- [2] V.N. Alekseev, D.I. Dmitriev, A.N. Zhilin, V.I. Reshetnikov, A.D. Starikov. Kvantovaya elektronika, 21 (8), 753 (1994) (in Russian).
- [3] V.N. Alekseev, V.N. Kotylev, V.I. Liber. Kvantovaya elektronika, **27** (3), 233 (1999) (in Russian).
- [4] V.N. Alekseev, V.I. Liber, A.D. Starikov. Patent RF №2040090 (1995) (in Russian).
- [5] G.N. Kachalin, A.F. Shkapa. *Sbornik dokladov vtoroi nauchnoi konferentsii "Molodezh" v nauke*" (Sarov, 2003), s. 437–440 (in Russian).
- [6] G.N. Kachalin, S.N. Pevnyi, D.N. Pivkin, A.S. Safronov. Kvantovaya elektronika, 42 (7), 677 (2012) (in Russian).
- [7] A.M. Dudov, S.M. Kulikov, A.V. Ryadnov, A.B. Smirnov, S.A. Sukharev. *Sbornik tezisov dokladov vtorogo vs-esoyuznogo simpoziuma po radiatsionnoi plazmodinamike* (M., 1991), ch. 3, s. 114–115 (in Russian).
- [8] G. Brederlov, E. Fill, K. Vitte. *Moshchnyi iodnyi lazer* (Energoatomizdat, M., 1985) (in Russian).
- [9] V.P. Arzhanov, B.L. Borovich, V.S. Zuev, V.M. Kazanskii, V.A. Katulin, G.A. Kirillov, S.B. Kormer, Yu.V. Kuratov, A.I. Kuryapin, O.Yu. Nosach, M.V. Sinitsin, Yu.Yu. Stoilov. Kvantovaya elektronika, 19 (2), 118 (1992) (in Russian).
- [10] S.G. Garanin, Y.V. Dolgopolov, G.N. Kachalin, A.V. Kopalkin, S.M. Kulikov, S.N. Pevnyi, F.A. Starikov, S.A. Sukharev. Quant. Electron., 52 (3), 289 (2022).
- [11] V.N. Alekseev Ekologicheskie vesti №6. Spetsial'nyi vypusk rabot stipendiatov imennykh nauchnykh stipendii Gubernatora Leningradskoi oblasti za 2002–2004 g. "Ekologicheskaya bezopasnost" khraneniya radioaktivnykh otkhodov". (in Russian).
- [12] V.N. Alekseev, D.I. Dmitriev, V.I. Reshetnikov. Kvantovaya elektronika, 18 (1), 111 (1991) (in Russian).

Translated by M.Shevelev